

Synthesis and characterization of Mg/TiO₂ nano-composites for electrical resistivity

N. Aghababaei*

Department of Chemical Engineering, Tafresh University, Postal Code 39518-79611, Iran

Received March 24, 2016; Accepted August 8, 2016

Magnesium (Mg) matrix reinforced with TiO₂ particles, due to the good electrical and thermal conductivity and strength at high temperature are suitable for contact materials. In this work Mg /TiO₂ nano-composites with different concentrations of TiO₂, were synthesized using in-situ oxidation of Mg-Ti pre alloyed powders. The morphology of prepared nano-composite specimens were characterized using scanning electron microscope (SEM). X-ray diffraction (XRD) analysis was used to investigate the mechanical behavior of Mg and Ti powders mixture. The physical and mechanical properties results of specimens indicated that the density, specific electrical resistivity, hardness and wear rate values can change by enhancement in TiO₂-loaded Mg matrix.

Keywords: Metal- matrix composites; Mg/TiO₂; Electrical properties; Mechanical properties.

INTRODUCTION

Magnesium and its alloys due to the good castability, machinability, thermal stability, good damping characteristics, high specific mechanical properties and resistance to electromagnetic radiation have been used for various applications in automobile, aerospace, sports-related and electronics industries [1-2]. Addition of ceramic particulates such as SiC, nanoparticles (NPs) such as TiB₂, other nanomaterials such as carbon nanotubes (CNTs) and addition of nano/micron sized metallic particles such as Ti can simultaneously improve in strengths and ductility of the magnesium composites [3,5].

Both pure magnesium and titanium dioxide are biocompatible materials. Therefore it is necessary to study the mechanical properties of pure magnesium reinforced with TiO₂ nano-particulates [6,9]. Internal oxidation, as in-situ production route of oxide dispersion strengthened (ODS) materials, has been the subject of numerous investigations during the past decade. This process has two major benefits first, it can prevent the formation of external oxide scale and second, internal oxidation provides a method of introducing second phase particles into an alloy which can affect the mechanical and other properties of alloys [10,15]. Due to limited works on Mg/TiO₂ composite as materials used in electrical contacts, the present work concentrates on this system. Mg/TiO₂ nano-composites have been produced by in-situ internal oxidation of Mg-Ti alloyed powder. In order to

investigate the effect of various amounts of TiO₂ particles on the density, electrical conductivity, hardness and wear rate of Mg/TiO₂ nano-composites, the Ti values was selected at the range of 1-3 wt.%.

2. EXPERIMENTAL

2.1 Synthesis of Mg/TiO₂ nanocomposites

In the present study, >99.9% pure MgO and Ti powder (with average particle sizes of 10–20nm) were obtained from Sigma–Aldrich. MgO powder was used 6,12 and 18 g as an oxidant. At the first stage, elemental Mg and Ti powders were mechanically alloyed for 3 days in argon atmosphere. The stainless steel balls to powder weight ratios (BPR) and mill rotation speed were selected as 20:1, 10:1 and 250 rpm, respectively. The Ti content was in the range of 1-3 wt. % in Mg-Ti powder composition.

Following mechanical alloying, the Mg-Ti alloyed powder and MgO were milled for 40 h and 60 h under Argon atmosphere. To prevent oxidation of very fine powder particles, compacting was conducted in a hot press under 30MPa applied pressure at 400°C in glove box. Heating rate was considered as 5°C/min. Finally, the specimens were cooled down for 12 h.

2.2 Characterization tests

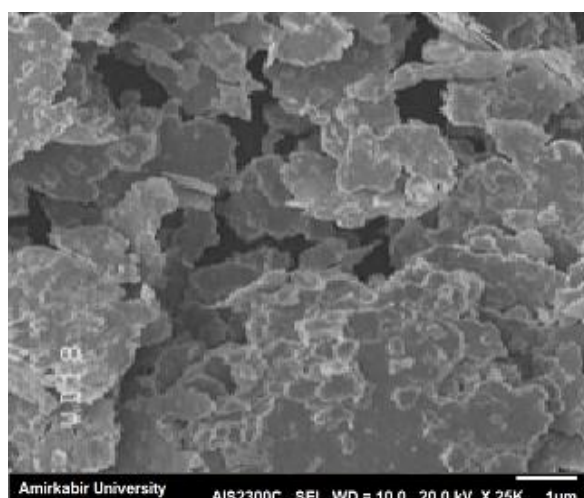
X-ray diffraction analysis was used to determine the mechanical alloying process during milling. The density value of specimens was specified by usual Archimedes method. The electrical resistivity was measured by micro-ohmmeter LOM-D500.

* To whom all correspondence should be sent:
E-mail: aghababaei@tafreshu.ac.ir

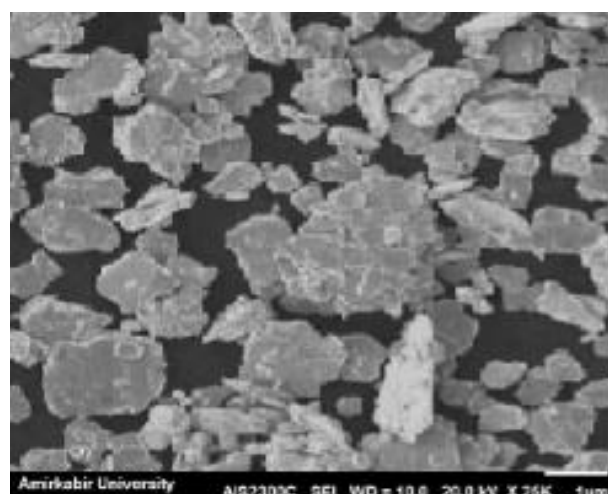
The specific electrical resistance were then calculated by considering specimens dimensions. The Vickers hardness was measured under applied load of 5 N. The weight loss was measured using a precise electronic balance. The wear rate was given as volume loss per unit sliding distance. To study the wear mechanisms of the specimens, worn surfaces of the pins were investigated using scanning electron microscope equipped with EDAX analysis.

3. RESULTS AND DISCUSSION

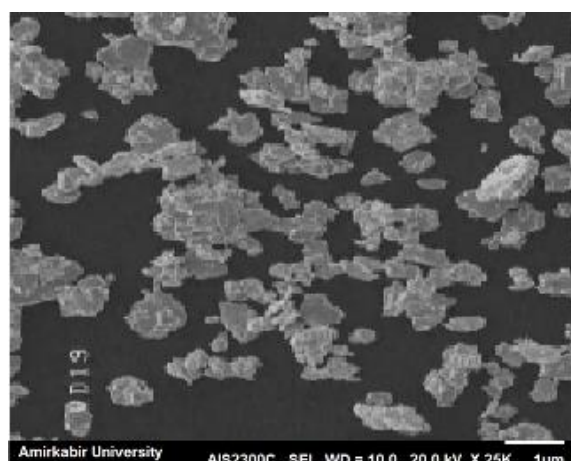
3.1. Characterization of Mg/TiO₂



(a)



(b)



(c)

Fig. 1 shows SEM micrographs of Mg-2wt.% Ti powder milled at different conditions. In fact, the flaky powder particles in Fig.1a and 1b, indicated that more time was required to reach a proper state between cold welding and fracturing of powder particles. Milling in 60 hr 20:1 did not decrease average particle size. A decrease in powder particle size and formation of thin layers between different particles made the atoms diffusion path shorter. As shown in Fig 1c, the particle size of powders milled for 60 hours with BPR 20:1 was less.

X-ray diffraction (XRD) was also applied to the Mg-Ti alloyed powders after 60 hr with BPR 10:1 and 20:1. The XRD results of Mg-2wt. % Ti powder after mechanical milling in different conditions are shown in Fig. 2.

The intensity of the peaks was decreased by increasing of BPR. Determination of crystallite size and lattice strain from the XRD data and using the

Williamson-Hall equation [9], confirms this change. XRD peaks of alloyed Mg should be shifted to lower θ values. However, due to low difference in atomic radii of Mg and Ti, the displacement of peaks is very negligible. In addition, dissolving of limited amounts of oxygen atoms and their placement on interstitial sites of Mg lattice would lead to strong decrease of lattice

parameter due to large difference in the atomic radii [16,18].

The XRD results of pressed and sintered specimens are illustrated in Fig.2. The intensity increment of the peaks is also sensible. However, due to very low amount of TiO₂ and small particle size, the diffraction peaks of TiO₂ are not appeared for this specimen.

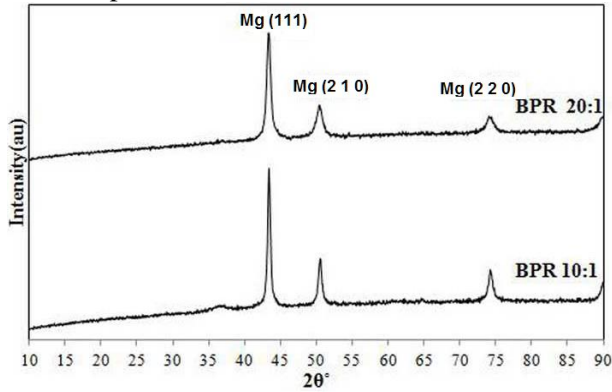


Fig.2. XRD analysis of Mg-2wt.% Ti powder after mechanical milling of 60 hrs with BPR 10:1 and 20:1.

Based on SEM image of Mg/TiO₂ nano-composite, the average grain size was about 50 nm (Fig.3). As shown the uniform particle size of Mg/TiO₂ was produced.

3.2. Specific electrical resistivity

The physical and mechanical properties of pressed and sintered specimens are presented in Tables 1 and 2. As shown, due to presence of Ti in Mg lattice and formation of solid solution, remained porosity, presence of MgO and probably some TiO₂ particles, specific electrical resistivity of pressed specimens increases with increasing Ti

content. In general, the values are higher than that pure Mg which is equal to 1.894 μΩ.cm. The specific electrical resistivity of Mg/TiO₂ composites was increased by increasing the amount of TiO₂ particles. Similar trends were obtained by other researchers [19, 20].

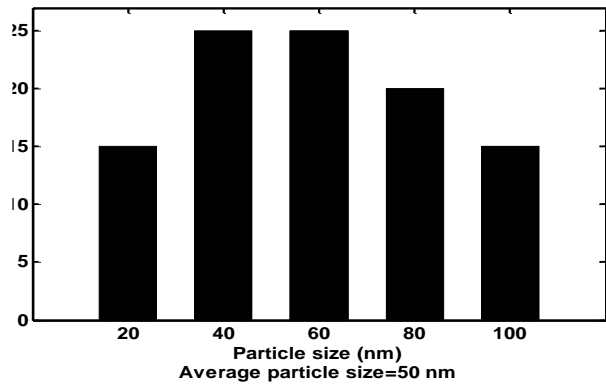
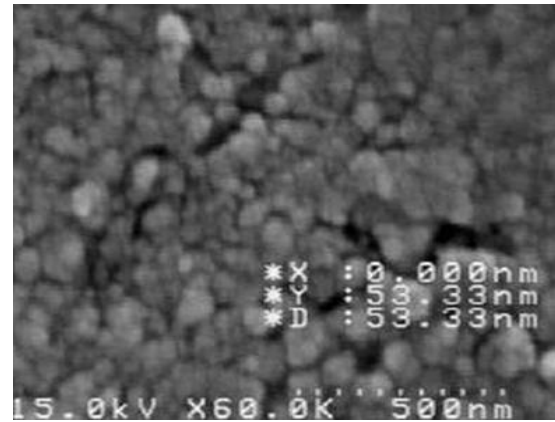


Fig.3. SEM image and particle size distribution of Mg/TiO₂.

Table 1. Properties of pressed specimens

Specimen Designation	Density (g/cm ³)	Specific electrical resistivity (μΩ.cm)
Mg/TiO ₂ 1	7.2	3.34
Mg/TiO ₂ 2	7.05	5.92
Mg/TiO ₂ 3	6.83	7.22

Table 2. Properties of sintered specimens

Specimen Designation	Density (g/cm ³)	Specific electrical resistivity (μΩ.cm)	Hardness (HV)
C1S	7.74	1.95	75.3
C2S	7.31	2.79	87.8
C3S	7.11	7.19	96.5

3.3. Vickers hardness

Vickers hardness of Mg/TiO₂ nano-composite samples are presented in Table 2. As shown, vickers hardness of Mg/TiO₂ nano-composite was increased by increasing TiO₂ amount. Two important strengthening and hardening mechanisms can be considered in the Mg/ TiO₂ nano-composite

produced by in-situ oxidation: the oxide dispersion strengthening according to orowan mechanism and refined grains strengthening according to Hall-Petch relation [19].

3.4. EDAX analysis

The EDS analysis of Mg/TiO₂, confirmed that elemental such as Ti, Fe and O can be detected

besides the main element Mg. According to the Table 3, the oxygen and iron content were increased by increasing sliding distance. Thus it can be

concluded that the oxidation wear mechanism becomes more activated at larger distances.

Table 3. EDS analysis of Mg/TiO₂ specimen after sliding of 3000 m

Element	Unn. C[wt.-%]	Norm. C	[at.-%]
Oxygen	0.65	0.75	2.89
Titanium	1.82	1.89	2.49
Iron	2.33	2.68	2.97
Mg	93.74	94.68	91.65

4. CONCLUSION

The effect of Ti content on the formation of in-situ TiO₂ particles in Mg matrix composites and evaluation of some physical and mechanical properties revealed that the formation of TiO₂ particles can be proceeded by mechanical milling and subsequent sintering of Mg (Ti)-MgO powders mixture. SEM image indicated that the uniform particles with average size of 50 nm were successfully synthesized. Specific electrical resistivity and hardness of Mg/TiO₂ nano-composites was increased with increasing oxide particles content.

REFERENCES

1. C. Goh, M. Gupta, Wei J., Lee L., *J Compos Mater*, **42**, 2039 (2008).
2. I. Itoi, K. Takahashi, H. Moriyama, M. Hirohashi, *Scripta Mater.*, **59**, 1155 (2008).
3. M. Gupta, M. Lai, *J. Mater. Sci.*, **35**, 2155 (2000).
4. G.K. Meenashisundaram, S. Sankaranarayanan, M. Gupta, *Mater. Charact.*, **94**, 178 (2014).
5. C. Goh, Wei J, Lee L, M. Gupta, *Compos. Sci. Technol.*, **68**, 432 (2008).
6. M.H. Nai, Wei J., M. Gupta, *Mater. Des.*, **60**, 490 (2014).
7. G.K. Meenashisundaram, M. Gupta, *J. Alloy Compd.*, **593**, 176 (2014).

8. G. Karunakaran, R. Suriyaprabha, P. Manivasakan, R. Yuvakkumar, V. Rajendran, N. Kannan, *Ecotoxicol. Environ. Safety*, **93**, 191 (2013).
9. H. Khoshzaban Khosroshahi, F. Fereshteh Saniee, H. Abedi, *Mater. Sci. Eng. A*, **595**, 284 (2014).
10. A.B. Moldes, R. Paradelo, D. Rubinos, R. Devesa-Rey, J.M. Cruz, M.T. Barral., *J. Agric. Food Chem.*, **59**, 9443 (2011).
11. N. Stanford, D. Atwell, A. Beer, C. Davies, M. Barnett, *Scripta Mater.*, **59**, 772 (2008).
12. S. Jayalakshmi, S. Sankaranarayanan, S. Koh, M. Gupta, *J. Alloy Compd.*, **565**, 56 (2013).
12. S. Seetharaman, J. Subramanian, K.S. Tun, A.S. Hamouda, M. Gupta, *Materials*, **6**, 1940 (2013).
13. G. Garcés, M. Rodríguez, P. Perez, P. Adeva, *Mater. Sci. Eng., A*, **419**, 57 (2006).
14. G. Garcés, P. Pérez, P. Adeva, *Scripta Mater.*, **52**, 615 (2005).
15. M.K. Habibi, S.P. Joshi, M. Gupta, *Acta Mater.*, **58**, 6104 (2010).
16. Wang X., Wu K., Zhang H., Huang W., Chang H., Gan W., et al., *Mater Sci Eng, A*, **465**, 78 (2007).
17. J. González-Benito, E. Castillo, J. Caldito, *Eur. Polymer J.*, **49**, 1747 (2013).
18. H. Dieringa, *J. Mater. Sci.*, **46**, 289 (2011).
19. C. Goh, Wei J., Lee L., M. Gupta, *Acta Mater.*, **55**, 5115 (2007).
20. K. Tun, P. Jayaramanavar, Nguyen Q., Chan J., Kwok R., M. Gupta, *Mater. Sci. Technol.*, **28**, 82 (2012).

